



## Photocatalytic degradation of methyl orange using doped ZnO nanocatalyst

D. K. Bhole, R. G. Puri, P. D. Meshram and R. S. Sirsam\*

University Institute of Chemical Technology, Kavayitri Bahinabai Chaudhari North Maharashtra University, Jalgaon-425 001, Maharashtra, India

E-mail: rajkumarsirsam@gmail.com

Manuscript received online 20 December 2019, revised and accepted 04 January 2020

Photocatalysis has been emerged as a potential solution for the degradation of organic compounds present in wastewater. Zinc oxide (ZnO) possess broad band gap (3.2 eV) absorbing more light quanta to be effective for degradation of organic pollutants. In present work, pure ZnO nanoparticles were synthesized by precipitation method involving dropwise addition and instant addition of zinc acetate dihydrate solution in sodium bicarbonate at different temperature. Alkaline earth metal magnesium (Mg) and transition metal manganese (Mn) were doped with pure ZnO nanoparticles to enhance the photocatalytic degradation rate. The characterization of synthesized nanocatalyst was carried out using XRD, FE-SEM and FTIR. The degradation performance of methyl orange (MO) in the presence of pure ZnO, Mg-ZnO and Mn-ZnO nanocatalyst were carried out in batch reactor by UV irradiation. Degradation efficiency of 90.2% and 85.8% were observed for Mg-ZnO and Mn-ZnO nanocatalyst at neutral pH, 150 mg of catalyst loading and 1000 ppm MO concentration, respectively.

Keywords: Photocatalysis, degradation, methyl orange, doping, nanocatalyst.

### Introduction

Textile sector has made a major contribution to the national economy. Textile industries discharge a large amount of dyeing effluent which is resistant to biological degradation and may require longer degradation time. This led to immediate attention in treatment of textile effluent before its discharge it into water bodies. For the complete annihilation of contaminants, advanced oxidation processes (AOPs) have emerged as a promising effluent treatment technology<sup>1</sup>. However, AOPs have inherent limitations of high capital cost, operating and maintenance cost, difficulty in removal of chemical reagents used<sup>2-4</sup>. On the contrary, use of novel photocatalysis process offer potential solution in treatment of wastewater resulting into complete mineralization of organic compounds present with higher efficiency<sup>5</sup>. Many types of semiconductors including TiO<sub>2</sub><sup>6</sup>, BiVO<sub>4</sub><sup>7</sup>, SnO<sub>2</sub><sup>8</sup>, CeO<sub>2</sub><sup>9</sup> have been studied as photocatalyst due to their high photosensitivity, non-toxic nature, low cost and chemical stability. However, applications of TiO<sub>2</sub> are limited because of its narrow photocatalytic range ( $\alpha < 400$  nm) and its ability to absorb only a small fraction (5%) of incident solar irradiation<sup>10</sup>.

In recent years, ZnO nanoparticles have appeared to be a suitable alternative for TiO<sub>2</sub> in photocatalytic degradation due to its large band gap of  $\sim 3.37$  eV and high efficiency<sup>11</sup>. Also, it absorbs a large fraction of the solar spectrum and more light quanta than TiO<sub>2</sub><sup>12</sup>. The method to prepare ZnO nanoparticles is very well established<sup>13</sup> and its photocatalytic activity was improved using many reformative methods such as doping of transition metal ions<sup>14-16</sup>, a combination of narrow band gap semiconductors<sup>17</sup> and aggradation of noble metals<sup>18,19</sup>. Doping has been reported to establish an equilibrium barrier between the photocatalyst and metal deposits without influencing reaction mechanism<sup>20</sup>. Nevertheless, doping favors electron-hole separation that enhances photocatalytic efficiency of metal oxide nanocatalyst<sup>21</sup>.

Here, we report synthesis of ZnO nanoparticles and its doping with transition metal Mn and alkaline earth metal Mg. The impact of various process parameters such as pH, photocatalyst (ZnO) loading, concentration of methyl orange (MO) and the efficiency of Mg-ZnO and Mn-ZnO on the degradation of MO has been discussed.

## Experimental

### Materials:

Zinc acetate dihydrate [Zn(Ac)<sub>2</sub>·2H<sub>2</sub>O], manganese acetate tetrahydrate [(Ac)<sub>2</sub>Mn·4H<sub>2</sub>O] and Tween-20 were obtained from Merck specialties Pvt. Ltd. Sodium bicarbonate (NaHCO<sub>3</sub>) and magnesium nitrate hexahydrate [Mg(NO<sub>3</sub>)<sub>2</sub>·6H<sub>2</sub>O] were procured from Qualigens Fine Chemicals. All reagents were of analytical grade and used as received.

### Preparation of catalyst:

ZnO nanoparticles were synthesized by drop-by-drop addition of zinc acetate dihydrate solution to sodium bicarbonate solution at 20°C, 35°C and 50°C with vigorous stirring<sup>22</sup>. In instant addition method, sodium bicarbonate solution was added under vigorous stirring in sodium bicarbonate solution at 35°C. The resultant reaction mixture was filtered, water washed several times and dried followed by calcination at 200°C for hold time of 3 h. Drop-by-drop addition method was used in synthesis of doped nanocatalyst viz. Mg-ZnO and Mn-ZnO wherein [Mg(NO<sub>3</sub>)<sub>2</sub>·6H<sub>2</sub>O] and [(Ac)<sub>2</sub>Mn·4H<sub>2</sub>O] solutions were added to the solution of sodium bicarbonate in presence of zinc acetate dihydrate.

### Photocatalytic reactor and experimental procedure:

A batch reactor (L, 38.1 cm×Ø, 9 cm) of borosilicate glass was used for photocatalytic degradation study. Synthetic effluent of MO solution and pre-determined quantity of doped ZnO nanocatalyst was taken in batch reactor and subjected to aeration to achieve uniform mixing. In order to achieve the activation of ZnO nanocatalyst, a UV lamp of 8 W (wavelength of 365 nm, intensity of 720 µW/cm<sup>2</sup> at 15 cm) was placed at the center of reactor. The reaction mixture pH adjustment in the range of 2–12 was done using dilute solutions of NaOH and H<sub>2</sub>SO<sub>4</sub>. At specific time interval, reaction mixture sample was withdrawn, centrifuged and filtered to recover nanocatalyst. The filtrate was analyzed for residual MO concentration, using UV-Vis spectrophotometer (Hitachi U-2900) to yield quantitative degradation of MO.

## Results and discussion

### UV-Vis spectrophotometry:

Optical properties of synthesized ZnO, Mg-ZnO and Mn-ZnO nanocatalyst were estimated from their UV absorbance

and are given in Table 1. After doping, Mg-ZnO and Mn-ZnO catalyst exhibited shift in absorption edge to the longer wavelength (redshift). This behavioral redshift caused decrease in band gap energy values from 3.44 eV (ZnO) to 3.39 eV (Mg-ZnO) and 3.42 eV (Mn-ZnO). Such reduction in band gap is due to strong quantum mechanical effects that enhance the surface area to volume ratio of doped catalyst<sup>21</sup>.

**Table 1.** Optical properties of pure ZnO, Mg-ZnO and Mn-ZnO nanocatalyst

Catalyst	$\lambda_{\max}$ (nm)	Band gap (eV)
Pure ZnO	360	3.44
3 wt% Mg-ZnO	366	3.39
3 wt% Mn-ZnO	362	3.42

### X-Ray diffraction analysis:

X-Ray (D8 Bruker, Germany) diffraction patterns of pure ZnO nanoparticles are shown in Fig. 1(a). All the patterns showed a hexagonal wurtzite crystal structure, which is assigned by comparing the diffraction peak position with the international crystallographic data table for standard ZnO powder<sup>23</sup>. The intensity of ZnO diffraction peaks for nanoparticles synthesized at 20°C and 35°C shows greater crystallinity and sharp peaks than for nanoparticles synthesized at 50°C and by instant addition method at 35°C. Fig. 1(b) showed that the Mg-ZnO nanocatalyst has hexagonal wurtzite crystal structure similar to pure ZnO, whereas Mn-ZnO nanocatalyst shows a cubic crystal structure. It has been reported that the smaller crystallite size induced a larger band gap due to increased redox ability and this quantum size effect enhances its photocatalytic activity<sup>24,25</sup>. Observations revealed good crystallinity for ZnO and Mg-ZnO nanocatalyst than Mn-ZnO nanocatalyst.

### Scanning electron microscopy:

Micrographs of pure ZnO synthesized at different temperatures were recorded on S4800 scanning electron microscope (Hitachi) and are shown in Fig. 2(a-d). ZnO nanoparticles are observed to be hexagonal but nearly spherical. Synthesis temperature of 50°C resulted to yield lesser agglomerated ZnO and has size less than 50 nm. ZnO nanoparticles synthesized by instant addition method [Fig. 2(d)] shows relatively larger particle size than drop wise ad-

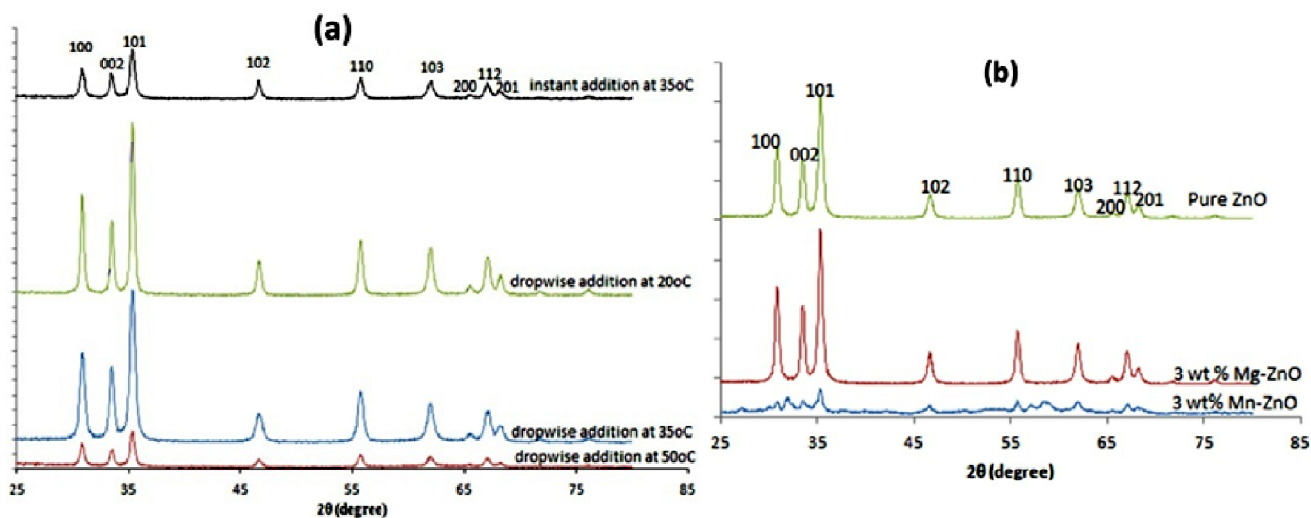


Fig. 1. XRD pattern of (a) ZnO nanocatalyst and (b) pure ZnO, Mg-ZnO and Mn-ZnO nanocatalyst.

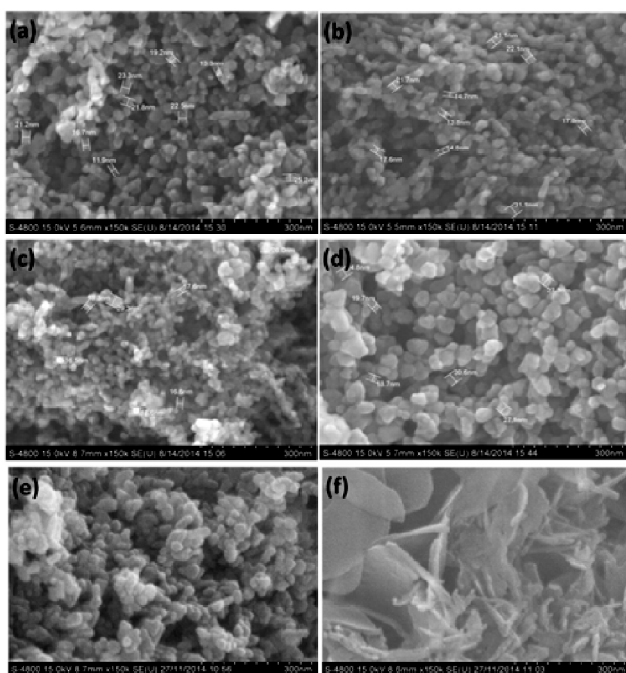


Fig. 2. SEM micrographs of ZnO nanocatalyst (a) dropwise addition at 35°C, (b) dropwise addition at 50°C, (c) dropwise addition at 20°C, (d) instant addition at 35°C, (e) Mg-ZnO and (f) Mn-ZnO nanocatalyst.

dition method. Similarly, surface morphology of 3 wt% Mg-ZnO and Mn-ZnO nanocatalyst were obtained using SEM [Fig. 2(e,f)]. It was observed that Mg-ZnO nanocatalyst is nearly spherical in shape with agglomeration, whereas Mn-ZnO nanocatalyst has flaked like morphology.

*Fourier transform infrared (FT-IR) spectroscopy:*

Functionality of ZnO, Mg-ZnO and Mn-ZnO nanocatalyst was examined using FT-IR (FTIR-8400 Shimadzu). Fig. 3(a) shows the IR spectrum of ZnO, where band located at 523.69  $\text{cm}^{-1}$  is attributed to the Zn-O stretching mode. In case of Mg-ZnO nanocatalyst, the band at 1435.55  $\text{cm}^{-1}$  corresponds to Mg-O stretching vibration [Fig. 3(b)]. The band at 1442.08  $\text{cm}^{-1}$ , 677.04  $\text{cm}^{-1}$  [Mg-ZnO, Fig. 3(b)] and 947.8  $\text{cm}^{-1}$ , 700.18  $\text{cm}^{-1}$  [Mn-ZnO, Fig. 3(c)] confirm composites of doped ZnO.

*Degradation study of MO:*

*Effect of ZnO photocatalyst:*

Three different sets of experiments were performed for

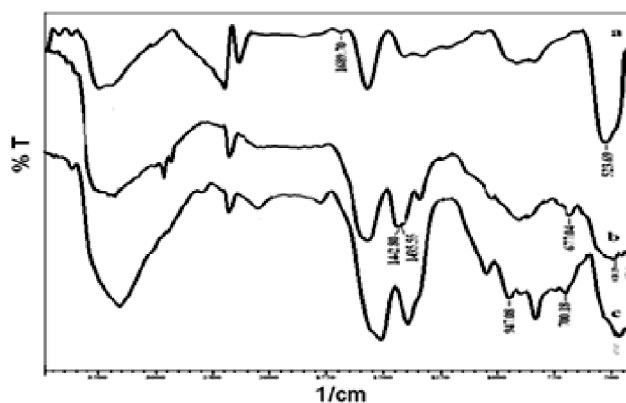


Fig. 3. FT-IR spectra of (a) pure ZnO, (b) Mg-ZnO and (c) Mn-ZnO nanocatalyst.

the confirmation of MO degradation by ZnO photocatalyst in presence of UV light. MO solution (1000 ppm) exposed to degrade by addition of 150 mg ZnO in presence and absence of UV irradiation at neutral pH. Blank experiment was performed to confirm the degradation of MO in absence of ZnO. Fig. 4(a) shows that 74% degradation of MO could be

achieved in 4 h of UV irradiation.

*Effect of ZnO photocatalyst loading:*

Catalyst loading plays a vital role in the photocatalytic degradation. Experiments were performed at increasing amount of ZnO to study its effect on degradation rate. Fig. 4(b) indicates that at higher catalyst loading of 150 mg of

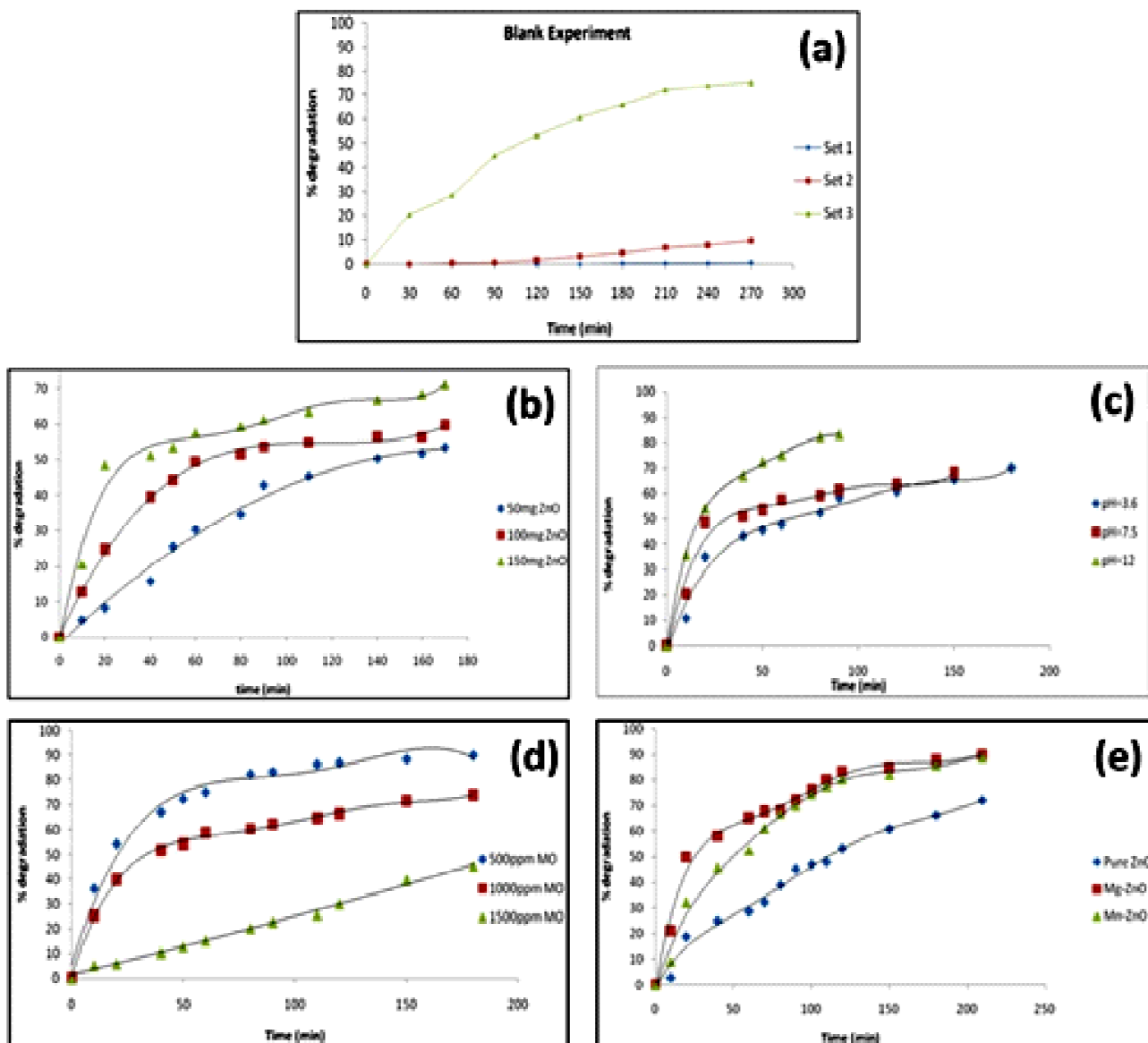


**Fig. 4.** (a) MO degradation runs: Set 1 (UV source - No, MO concentration - 1000 ppm, ZnO loading - 150 mg, pH - Neutral), Set 2 (UV source - Yes, MO concentration - 1000 ppm, ZnO loading - No, pH - Neutral), Set 3 (UV source - Yes, MO concentration - 1000 ppm, ZnO loading - 150 mg, pH - Neutral); (b) Effect of ZnO nanocatalyst percent degradation of MO (MO concentration - 1000 ppm, pH - Neutral); (c) Effect of pH on percent degradation of MO (MO concentration - 1000 ppm, ZnO loading - 150 mg); (d) Effect of initial concentration on percent degradation of MO (ZnO loading - 150 mg, pH - Neutral) and (e) Effect of Mn-, Mg-doping on percent degradation of MO (MO concentration - 1000 ppm, ZnO loading - 150 mg, pH - Neutral).

ZnO shows significantly better results than with 50 mg and 100 mg of loading. It infers that the degradation efficiency increases with increase in photocatalyst loading as ability of catalyst to adsorb and form the active species ultimately increases. At higher catalyst loading (>150 mg), increase in suspension turbidity was observed, which may affect penetration of UV light. Hence, further experiments with higher catalyst loading were not performed.

#### Effect of pH:

The solution pH plays an important role in photodegradation process. Also, pH is dependent on surface charge of photocatalyst. Fig. 4(c) demonstrates the effects of pH on the degradation of MO at similar operating conditions. It was observed that acidic medium is unfavorable for photocatalysis because of the dissolution of ZnO. In acidic medium, H<sup>+</sup> ions are produced which declines the degradation rate. At higher pH values (alkalinity), although OH<sup>-</sup> ions are produced which supports the reaction, the time for degradation is increased due to repulsion between much negatively charged catalyst surface and dye anions. Although, basic pH shows higher degradation rate, but due to excessive deposition of Na<sup>+</sup>, it was decided to conduct experiments at optimized pH of 7.5.

#### Effect of MO concentration:

Fig. 4(d) represents effect of MO concentration on the degradation rate at otherwise similar operating conditions. It was quite predictable that the degradation gradually decreases with increase in MO concentration. As usual, this is because the increased concentration of dye results in a deep colored solution which decreases UV light penetration. This supports the degradation percentage of 90% at 500 ppm and 74.2% at 1000 ppm obtained after 180 min of UV irradiation.

#### Effect of doping on degradation rate of MO:

Enhancement in photocatalytic efficiency was studied with doping impact of transition and alkaline earth metal atoms on the surface of ZnO. Fig. 4(e) represents percentage degradation of MO using ZnO, Mg-ZnO and Mn-ZnO photocatalyst. Degradation of MO was found to be in the descending order of Mg-ZnO > Mn-ZnO > ZnO. This shows that doping has improved degradation ability of ZnO in its pure form. Among doped ZnO, Mg-ZnO was superior to Mn-ZnO. Doping with Mg salt resulted into higher reduction in band gap energy than with Mn salt. In addition, Mg-ZnO has better

crystallinity than Mn-ZnO. This caused effective electron-hole separation in Mg-ZnO catalyst, responsible for its photocatalytic effectiveness.

### Conclusions

Pure ZnO and (Mg, Mn) doped ZnO nanocatalyst were successfully synthesized by precipitation method to serve as photocatalyst for the degradation of MO. Photocatalytic activity of Mg-ZnO and Mn-ZnO nanocatalyst confirmed rapid degradation of MO than the pure ZnO. This is due to their available large surface area, which improves charge separation between photogenerated electron and holes. Mg-ZnO nanocatalyst was more effective for photodegradation of MO in aqueous solution under UV source. The maximum degradation of 90.2% and 85.8% was achieved for Mg- and Mn-doped ZnO, respectively.

### References

1. M. I. Franch, J. A. Ayllón and X. Domènech, *Appl. Catal. B: Environ.*, 2009, **50**, 89.
2. S. H. Lin and R. S. Juang, *J. Environ. Manage.*, 2009, **90**, 1336.
3. S. Wang and Y. Peng, *Chem. Eng. J.*, 2010, **156**, 11.
4. P. Patil, G. Gaikwad, D. Patil and J. Naik, *Bull. Mater. Sci.*, 2016, **39**, 655.
5. Yi, C. Lu, Ch. Chiing-Chang and Lu Chung-Shin, *J. Taiwan Inst. Chem. Eng.*, 2014, **45**, 1015.
6. A. Heller, *Acc. Chem. Res.*, 1995, **28**, 503.
7. K. Pingmuang, J. Chen, W. Kangwansupamonkon, G. G. Wallace, S. Phanichphant and A. Nattestad, *Scientific Reports*, 2017, **7**(1), 8929.
8. B. Liu, X. Liu, M. Ni, C. Feng, X. Lei, C. Li, Y. Gong, L. Niu, J. Li and L. Pan, *Applied Surface Science*, 2018, **453**, 280.
9. D. Channei, B. Inceesungvorn, N. Wetchakun, S. Ukritnukun, A. Nattestad, J. Chen and S. Phanichphant, *Scientific Reports*, 2014, **4**, 5757.
10. A. L. Linsebigler, G. Lu and J. T. Yates, *Chem. Rev.*, 1995, **95**, 735.
11. C. Chen, J. Liu, P. Liu and B. Yu, *Adv. Chem. Eng. Sci.*, 2011, **1**, 9.
12. S. Sakthivel, B. Neppolian, M. V. Shankar, B. Arabindoo, M. Palanichamy and V. Murugesan, *Sol. Energy Mater. Sol. Cell*, 2003, **77**, 65.
13. D. Sridevi and K. V. Rajendran, *Bull. Mater. Sci.*, 2009, **32**, 165.
14. A. V. Rupa, D. Manikandan, D. Divakar and T. Sivakumar, *J. Hazard. Mater.*, 2007, **147**, 906.
15. N. Sobana, M. Muruganadham and M. Swaminathan, *J. Mol. Catal. A: Chem.*, 2006, **258**, 124.
16. K. Chaing, T. M. Lim, L. Tsen and C. C. Lee, *Appl. Catal.*

Bhole *et al.*: Photocatalytic degradation of methyl orange using doped ZnO nanocatalyst

- A: General*, 2004, **261**, 225.
17. P. V. Kamat, *Chem. Rev.*, 1993, **93**, 267.
  18. A. Wold, *Chem. Mater.*, 1993, **5**, 280.
  19. A. Sclafani and J. M. Herrmann, *J. Photochem. Photobiol. A: Chem.*, 1998, **113**, 181.
  20. W. Y. Teoh, J. A. Scott and R. Amal, *J. Phys. Chem. Lett.*, 2012, **3**, 629.
  21. S. Khajuria, S. Sanotra, J. Ladol and H. N. Sheikh, *Journal of Materials Science: Materials in Electronics*, 2015, **26(9)**, 7073.
  22. N. Clament Sagaya Selvam, S. Narayanan, L. John Kennedy and J. Judith Vijaya, *J. Environ. Sci.*, 2013, **25**, 2157.
  23. J. M. Wang and L. Gao, *J. Am. Ceram. Soc.*, 2005, **88**, 1637.
  24. D. S. Kim, S. J. Han and S. Y. Kwak, *J. Colloid Interface Sci.*, 2007, **316**, 85.
  25. A. R. Liu, S. M. Wang, Y. R. Zhao and Z. Zheng, *Mater. Chem. Phys.*, 2006, **99**, 131.
  26. K. I. Hadjiivanov and D. K. Klissurski, *Chem. Soc. Rev.*, 1996, **25**, 61.
  27. N. Serpone, D. Lawless, J. Disdier and J. M. Hermann, *Langmuir*, 1994, **10**, 643.